RSC Advances

ROYAL SOCIETY OF CHEMISTRY

www.rsc.org/advances

Journal Name

ARTICLE

Synthesis of 5A zeolite coating/PSSF composites for adsorption of methane from air

Dong Zhang, Huiping Zhang, Ying Yan*

Received 00th January 20xx,
Accepted 00th January 20xx

DOI: 10.1039/x0xx00000x

www.rsc.org/

To remove lean methane from air, adsorption process involving fixed-bed filled with small adsorbents is often used. This process, however, has some drawbacks such as large bed pressure drop and low bed utilization. To overcome these shortcomings, we fabricated novel 5A zeolite coating/paper-like sintered stainless steel fibers (PSSFs) composites by using in situ hydrothermal method on 3-aminopropyltrimethoxysilane-functionalized support. The composites have large external surface area and high voidage. They were further characterized by X-ray diffraction (XRD), scanning electron microscopy (SEM) and N2 adsorption/desorption. Moreover, we packed these composites in the end of fixed bed to form structured fixed beds and test adsorption dynamics. We analyzed breakthrough curves obtained from adsorption dynamics by length of unused bed model (LUB). Results showed that the composites were successfully prepared with dense coating. Furthermore, the breakthrough curves of structured fixed beds were steeper than that of the fixed bed. We concluded that by forming structured fixed beds with 5A zeolite coating/PSSF composites, the bed pressure drop could be reduced and the bed utilization could be improved.

1. Introduction

The emissions of methane, a potent greenhouse gas, are serious environmental issues[1]. How to reduce the methane emissions has become one of the major concerns among scientists. To eliminate the methane from air, catalytic combustion[2] and adsorption[3] are the commonly used methods. In conventional adsorption process, commercial adsorbents such as activated carbon[4], zeolites[5-7] of large particle sizes (more than 1mm) are usually packed in the fixed-bed adsorber. These large adsorbents, however, exhibit poor thermal conductivity, large inter-particle and intra-particle transport resistance, creating channeling and axial dispersion[8]. These effects prolong the mass transfer zone (MTZ) and reduce the overall bed utilization. As a result, we expect approaches to decrease the intra-particle and inter-particle resistances, increase mass transfer rates and improve the bed utilization.

A promising solution is the microfibrous material developed by Tatarchuk[8]. It is the matrix made of metal, glass, etc., that incorporates particles as small as 10μm. These particles could be adsorbents, catalyst, electrocatalyst and solid reactants. The materials own advantageous characteristics such as large external surface, high voidage, porosity, thermal/electrical conductivity. When applied into adsorption/catalysis operation, these materials could enhance both the external and intra-particle heat/mass transfer rate. For instance, microfibrous entrapped ZnO adsorbent outperformed 2-3 fold over the fixed bed reaction rates in the removal of H_2S [9]. Microfibrous entrapped Al_2O_3/Ni catalyst showed 2-6 times higher catalytic activities than fixed bed reactor with similar catalyst loading for the toluene hydrogenation[10]. Although the microfibrous materials prepared by Tatachurk showed great potential as adsorbents or catalysts, there are some shortcomings regarding these materials. To begin with, sintered nickel fibers, supports of the microfibrous materials, are expensive, leading to high manufacture cost. In addition, to be entrapped into the matrix, adsorbents/catalyst granules have to be crushed and sieved at the beginning. In this process, only a small fraction of granules meet the particle-size requirement. Most granules of other sizes, however, are no longer usable in this process and therefore wasted.

To solve these problems, we prepared a novel paper-like sintered stainless-steel fibers (PSSF) support by wet lay-up papermaking and sintering process[11]. The manufacture cost of PSSF is only 10% of the sintered nickel fibers by replacing nickel fibers with stainless-steel fibers. The PSSF support provides advantages like thermal conductivity, mechanical strength and anticorrosion quality. Most importantly, instead of entrapping ZSM-5 particle, Chen[11] synthesized ZSM-5 zeolite membrane on PSSF to form the composites of large external surface area. The zeolite loading was adjustable by changing synthesis parameters rather than filling more granule into the matrix. These composites exhibit promising adsorption/catalysis activity of removing VOCs[11, 12]. However, so far, ZSM-5 is the sole type of zeolite that is coated on the PSSF support. The advantageous characteristics of PSSF, hence, provide an impetus to preparing more kinds of zeolite coating on this support.

*Corresponding author. Tel./fax: +86 2087111975.
E-mail address: yingyan@scut.edu.cn (Y. Yan).

Among zeolites, Linde Type A (LTA) zeolite coating[13-15], membrane[16-19] and film[20] have received a lot of attention because of the high selectivity and uniform pore size distribution of 0.3-0.5nm. Moreover, Ca-LTA(5A) zeolite exhibits the adsorption capacity for methane under ambient condition[21]. Thus, it is interesting to fabricate 5A zeolite coating on the PSSF to obtain 5A zeolite/PSSF composites. Adding these composites in the end of the fixed bed, we can form structured fixed bed. We hypothesize that this structured fixed bed could enhance mass transfer rate and reduce bed pressure drop when removing methane from air.

Our objectives are to fabricate 5A zeolite/PSSF composites and examine the adsorption dynamics of methane in 5A zeolite/PSSF composites structured fixed bed.

2. Experimental

2.1. Materials

3-aminopropyltrimethoxysilane (APTMS) (≥97%, Aladdin Industrial Corporation); sodium hydroxide (≥96%, Nanjing Chemical Reagent Co., Ltd); sodium aluminate (Al_2O_3≥41%, Sinopharm Chemical Reagent Co., Ltd); LUDOX HS-30 colloidal silica (30% SiO_2 in water, Aldrich); toluene (99.5%, Hunan Hengyang Kaixin Chemical Co., Ltd); ethanol (99.7%, Sinopharm Chemical Reagent Co., Ltd); calcium chloride anhydrous (≥96%, Tianjin Kermel Reagent Co., Ltd).

Stainless steel fibers (diameter of 6.5μm, Huitong Advanced Materials Co., Ltd); methane in air(104ppm, Guangzhou Zhuozheng Air Co., Ltd); 4A zeolite (250-425 μm, Tianjin Kermel Reagent Co., Ltd); 5A zeolite (250-425 μm, Tianjin Kermel Reagent Co., Ltd)

2.2. Preparation of LTA/PSSF composites

Paper-like sintered stainless-steel fibers (PSSF) were prepared by using wet layup papermaking/sintering technique[11]: Stainless steel fibers (6.5μm in diameter, 2-3 mm in length) and cellulose with the weight ratio of 2:1 were added to 1L water and stirred vigorously for 10 min to form the uniform suspension. A circular paper precursor was obtained by filtering the suspension using wet lay-up process, pressing at 300kPa for 30min and drying in air at 105°C for 24h afterwards. The dried paper precursor was sintered at 1050°C in nitrogen for 30min to destroy cellulose and form paper-like sintered stainless steel fibers support. The PSSF support was then calcined in air at 550°C for 4h.

The PSSF support was pretreated with APTMS in toluene (3g APTMS solved in 100g toluene) in 200mL Teflon lined autoclave at 110°C for 1h. To investigate the possible function of APTMS, another PSSF support was not treated with APTMS as a blank .A clear, homogenous LTA synthesis solution with molar ratio of 50 Na_2O: 1Al_2O_3: 5SiO_2: 1000H_2O[16] was prepared by vigorously stirring sodium hydroxide, sodium aluminate and colloidal silica in deionized water for 2h at 50°C. The pretreated support was placed vertically in Teflon-lined autoclave which was filled with synthesis solution. After in situ hydrothermal synthesis at 60°C for 24h, the 4A zeolite/PSSF composites were washed with deionized water and dried in oven at 105°C overnight.

For the as-synthesized 4A zeolite/PSSF composites, the hydrothermal synthesis procedure was repeated 1-2 times to adjust the zeolite coating thickness and to investigate its influence on the morphology of the composites.

To obtain 5A zeolite/PSSF composites, 4A zeolite/PSSF composites were ion-exchanged using aqueous $CaCl_2$ solution of 0.5mol/L at 60°C for 5h. After that, 5A zeolite/PSSF composites were thoroughly washed with deionized water and sintered at 300°C for 4h in air.

2.3. Characterization

The microstructure and morphology of synthesized zeolite coating sample was examined with Zeiss 1550 field emission SEM. Before the analysis, an ultra-thin layer of gold was sprayed on the sample. The crystallographic characterization of zeolite coating was carried out with X-ray diffractometer (Bruker Co. D8 ADVANCE) using CuKα radiation at 40 kV and 40 mA. The specific surface area and pore size distribution of 4A zeolite/PSSF, 5A zeolite/PSSF composites and commercial zeolites were measured using ASAP 2020 analyzer (Micromeritics Instrument Co., Ltd) at 77K. Before the measurements, samples were degassed at 523K for 4h under vacuum.

2.4. Adsorption dynamics of methane in structured fixed bed

Adsorption dynamics of methane in fixed bed and structured fixed bed were evaluated by using a stainless steel tube (I.D.:20mm, length:150mm). The fixed bed was packed with granular 5A zeolite (250-425 μm) of 150mm, and the structured fixed bed was filled with zeolite granule of 120mm in the inlet and 5A zeolite/PSSF composites of 30mm in the outlet of the bed. The experiments were carried out at 298K at ambient pressure using methane/air mixture (104ppm) as the inlet gas with flow rate of 20mL/min. Outlet gas was analyzed by gas chromatography (Agilent 7890A, USA) equipped with a flame ionization detector (FID). Breakthrough curves were plotted by calculating the values of C/C_0 (where C was the current concentration and C_0 is the inlet concentration) versus cumulative time t.

3. Theory

The length of unused bed (LUB), suggested by Collins[22], reflects half of mass transfer zone. The LUB value is analyzed by using the following equation to calculate the experimental breakthrough curve data.

$$LUB = \left(1 - \frac{t_b}{t_s}\right) L \quad (1)$$

Where L corresponds to the bed length (cm), t_b is the time corresponding to breakthrough concentration C_b = 2 ppm, t_s is the stoichiometric time.

4.Results and discussion

strength of the PSSF support. The surface of the PSSF support shown in Fig.1(c) was coarse, which benefited anchoring the

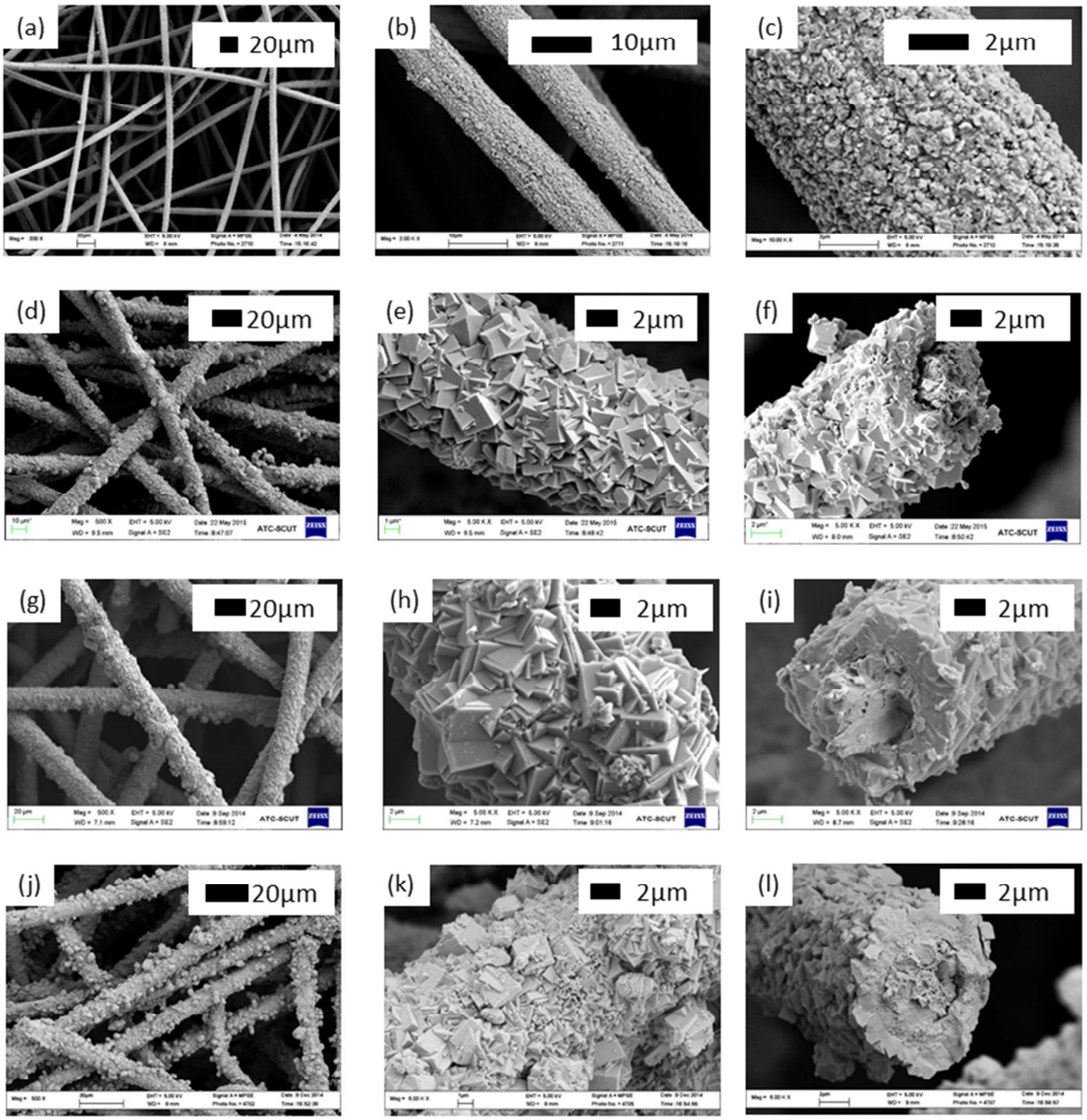

Fig. 1. SEM images of the PSSF support at 300x(a), 2kx(b) and 10kx(c); 4A zeolite/PSSF composites without APTMS treatment at 500x(d), 5kx(e), and its cross section at 5kx(f); 4A zeolite/PSSF composites with APTMS treatment at 500x(g), 5kx(h), and its cross section at 5kx(i); 5A zeolite/PSSF composites at 500x(j), 5kx(k), and its cross section at 5kx(l)

4.1. SEM morphology

The SEM characterization was used to investigate morphology and crystallinity of the PSSF support, 4A zeolite/PSSF composites with and without APTMS treatment, and 5A zeolite/PSSF composites. Fig.1(a) and (b) showed that 3-dimentional network structure enhanced the mechanical precursor of zeolite. The SEM images of 4A zeolite/PSSF composites without APTMS treatment in Fig.1(d), (e) and (f) showed that the LTA crystals assembled a dense and continuous layer on the PSSF support with a thickness of 1.5μm, without any visible cracks and other crystalline phases. In Fig.1(g), (h) and (i), the SEM images showed that the 4A

zeolite/PSSF with APTMS treatment was denser and the crystals are more interlocked in comparison with the one without APTMS treatment. The identical LTA zeolite coating of the same thickness was also seen in 5A zeolite/PSSF composites in Fig.1(j), (k) and (l).

In the present work, the methoxy groups of APTMS react with the hydroxyl groups on the surface of sintered stainless steel fibers in the pretreatment of the PSSF support. The silazane-based silylation reaction takes place between 3-aminopropylsiyl groups and silanol with ammonia release[16]. As a result, a "bridge" connects the support and the precursor of LTA zeolite, forming dense LTA zeolite coating on the support with in situ hydrothermal synthesis (Fig.2).

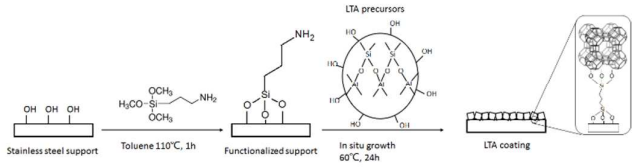

Fig.2. Scheme of the synthesis of LTA zeolite coating on the PSSF support using APTMS as covalent linker.

We also investigated the impact of synthesis times on the morphology of the composites. 4A zeolite/PSSF composites with APTMS treatment was then hydrothermally grown for 1-2 times. As can be seen in Fig.3, the interlocked LTA crystals appeared on both composites and no other type of zeolite crystals could be observed. The thickness of zeolite coating in the one of 2 hydrothermal times is nearly 3μm (Fig.3c) while that of the one of 3 hydrothermal times is almost 10μm (Fig.3f). It means that the thickness of zeolite coating increased with the hydrothermal synthesis times. Moreover, the coating tended to be unevenly distributed and many clusters were generated as the synthesis times increases.

4.2. XRD patterns

XRD was used to characterize the crystallinity of 4A zeolite/PSSF composites with APTMS treatment and 5A zeolite/PSSF composites. The XRD patterns of standard LTA zeolite (a), the PSSF support (b), 4A zeolite/PSSF composites with APTMS treatment (c) and 5A zeolite/PSSF composites (d) are presented in Fig.4.

Two intense diffraction peaks related to stainless steel fibers were shown at 2θ = 40–55° in XRD pattern of PSSF support (Fig.4b). One of the peaks was also identified in both 4A zeolite/PSSF composites (Fig.4c) and 5A zeolite/PSSF composites(Fig.4d). The absence of the peak at 2θ = 51° in Fig.4 (c) and (d) might be ascribed to the dense coating of 4A zeolite/PSSF composites. Besides, the diffraction peaks of 4A zeolite/PSSF composites and 5A zeolite/PSSF composites at the ranges of 5-40° corresponded with the standard LTA zeolite pattern. These results indicated that the LTA coating was synthesized on the PSSF support.

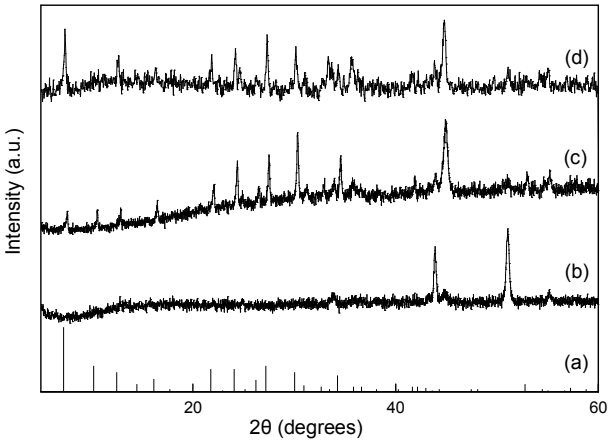

Fig.4. XRD patterns of standard LTA zeolite (a), the PSSF support (b), 4A zeolite/PSSF composites (c) and 5A zeolite/PSSF composites (d).

4.3. N_2 adsorption isotherms

N_2 adsorption isotherms were used to characterize the pore size distribution, BET surface area and pore volume of 4A

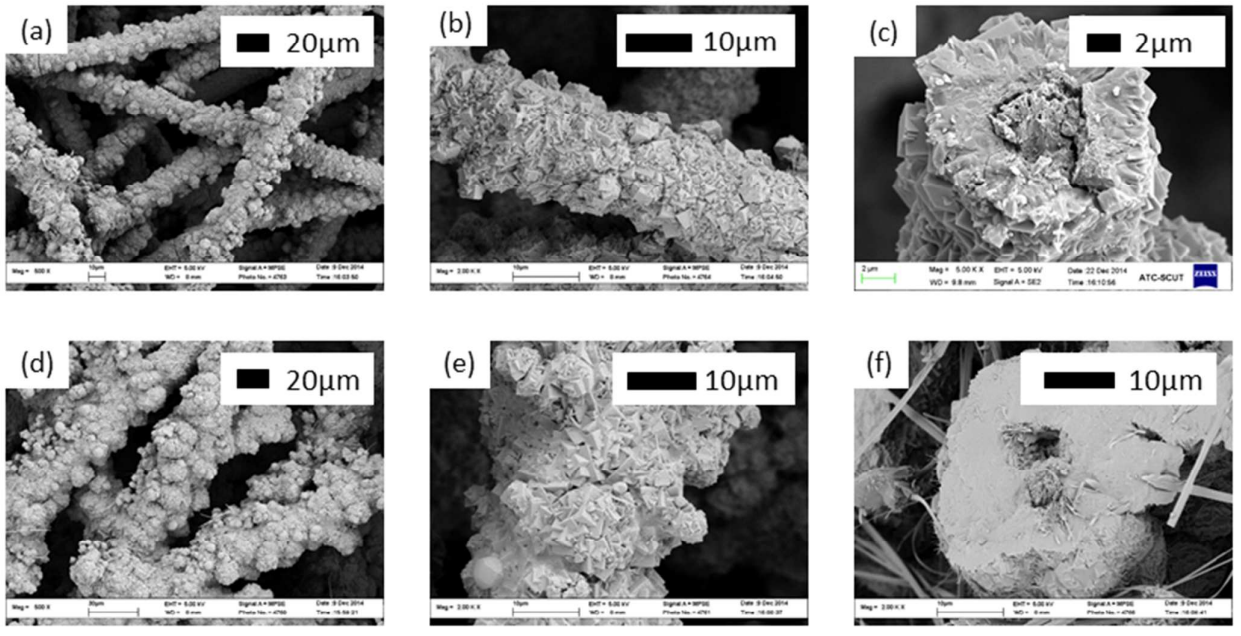

Fig.3. SEM images of 4A zeolite/PSSF composites with APTMS treatment hydrothermally grown for 2 times at 500x(a), 2kx(b) and the cross-section at 5kx(c); and hydrothermally grown for 3 times at 500x(a), 2kx(b) and the cross-section at 2kx(c).

zeolite/PSSF composites with APTMS treatment, 5A zeolite/PSSF composites and commercial zeolites. N_2 adsorption isotherms were taken at 77K by ASAP 2020. The samples were degassed at 523K for 4h under vacuum before the test. Micropore and mesopore size distribution of the samples was analyzed via DFT (Density Functional Theory) and BJH (Barret-Joyner-Halenda) method respectively. The micropore volume and the total pore volume was calculated via t-plot and single point method respectively. Besides, BET (Brunauer-Emmett-Teller) surface area was calculated from adsorption branches in the relative pressure range of 0.06-0.3.

As was shown in Table 1, the BET surface area and micropore volume of commercial 4A zeolite and 4A zeolite/PSSF composites was relatively low. This phenomenon might be explained by the poor adsorption of N_2 molecules at the pore openings[23, 24]. In comparison, the increase in BET surface area, micropore volume and total pore volume was observed in the sample of 5A zeolite/PSSF composites and commercial 5A zeolite, because of larger pore openings after ion-exchanged with Ca^{2+}. Besides, the micropore volume of 5A zeolite/PSSF composites of 1 hydrothermal time is much higher - 0.048 cm^3/g, 84% of the total volume than that of the commercial 5A zeolite.

N_2 adsorption isotherm of 5A zeolite/PSSF composites shown in Fig.5 was of type I, indicating the appearance of micropore structure. At the beginning of adsorption process, the volume adsorbed rises drastically as the relative pressure increases because the monolayer adsorption is achieved. The multilayer adsorption plays a key role as the relative pressure continues increasing. Furthermore, as can be seen in Fig.6, the pore size distribution of 5A zeolite/PSSF composites calculated via DFT theory proved the micropore structures as well. The micropore distribution was uniform and centered at about 0.5nm, which was in accordance with the theoretical pore size of 5A zeolite.

Besides, 5A zeolite/PSSF composites of 2 and 3 hydrothermal times showed higher surface area and micropore volume, which was the result of increased thickness of zeolite coating.

The results suggested that 5A zeolite/PSSF composites of different synthesis times had the micropore structure and was successfully prepared.

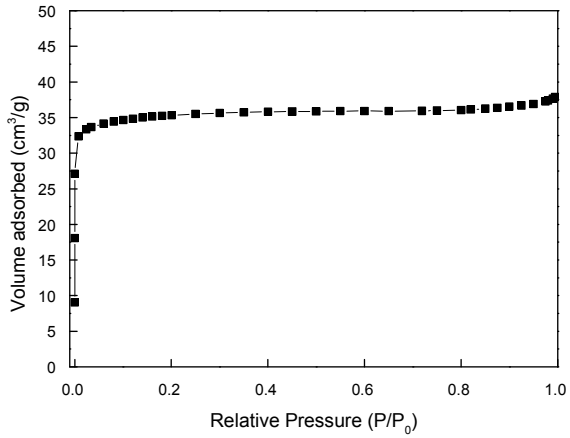

Fig.5. N_2 adsorption isotherm of 5A zeolite/PSSF composites at 77K.

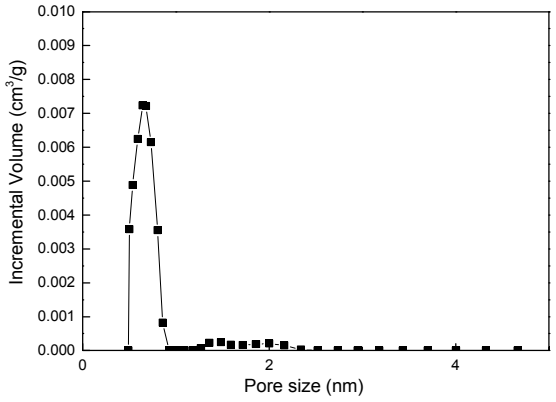

Fig.6. Pore size distribution of 5A zeolite/PSSF composites.

Table 1. Pore structure properties of PSSF support, commercial zeolites and composites.

Sample	Pore structure properties			
	Micropore (cm^3/g)	Mesopore (cm^3/g)	Total volume (cm^3/g)	BET Surface area (m^2/g)
PSSF	-	-	-	14
Commercial 4A zeolite	0.0024	0.052	0.044	20
4A zeolite/PSSF composites with APTMS treatment	-	-	-	0.31
Commercial 5A zeolite	0.15	0.071	0.21	375
5A zeolite/PSSF composites of 1 hydrothermal time	0.048	0.0064	0.057	118
5A zeolite/PSSF composites of 2 hydrothermal times	0.091	0.0053	0.092	178
5A zeolite/PSSF composites of 3 hydrothermal times	0.10	0.0061	0.12	188

4.4. Adsorption dynamics of methane

The differences in adsorption rate, mass transfer resistance in structured fixed beds and fixed bed were determined by analyzing adsorption dynamics.

The breakthrough experiments were carried out under the conditions of inlet methane concentration of 104ppm and flow rate of 20 mL/min. The fixed bed was filled with 5A zeolite granule (250-425 μm) of 150mm. The structured fixed bed was packed with granular 5A zeolite (250-425 μm) of 120 mm in the inlet and 5A zeolite/PSSF composites with different hydrothermal synthesis times of 30 mm in the outlet of the bed. For the structured fixed bed #1, #2 and #3, the composites were hydrothermally grown for 1,2 and 3 times before the ion-exchange procedure. Besides, we also tested the adsorption dynamics of 3cm-length 5A zeolite/PSSF composites of 1 hydrothermal time.

The experimental results were presented in Fig.7. The breakthrough curve of 5A zeolite/PSSF composites is more upright than others, representing its mass transfer rate is the highest. Although structured fixed beds exhibited less breakthrough time due to the lower adsorption capacity of 5A zeolite/PSSF composites, they owned a steeper breakthrough curve because structured fixed beds has less mass transfer resistance. Furthermore, the mass transfer zone of structured fixed beds was reduced in contrast to the fixed bed of the same length. These results suggested that the structured fixed beds had the superiorities of lower bed pressure drop, increased adsorption rate. When comparing the structured fixed beds with composites of different hydrothermal synthesis times, we found that the higher zeolite loading in the composites contributed by additional synthesis times increased the adsorption capacity. But it prolonged the mass transfer zone as well.

Therefore, we can conclude that 5A zeolite/PSSF composites enhance the mass transfer rate in structured fixed bed and higher zeolite loadings in the composites would not necessarily increase the mass transfer rate.

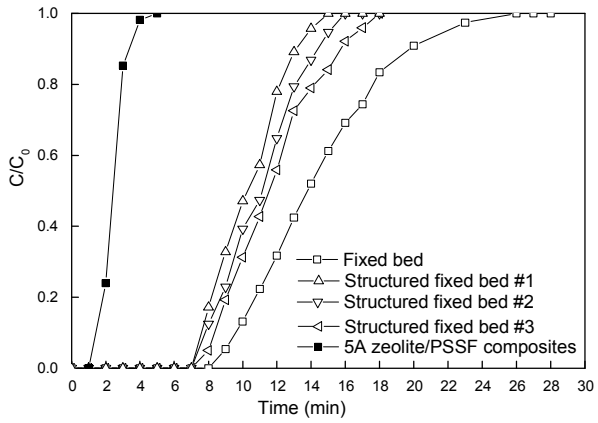

Fig.7. Breakthrough curves for methane adsorption on different beds.

4.5 Determination of Length of Unused Bed

It is of importance to increase the bed utilization by minimizing the length of unused bed (LUB) of fixed bed. The value was calculated from the breakthrough curve data according to Eq.(1), and results were shown in Table 2.

The LUB values of fixed bed and structured fixed bed #1 were 71.29 mm and 35.71 mm respectively. 5A zeolite/PSSF composites in the structured fixed bed #1 contributed to the decrease of 35.58 mm. Likewise, the ΔZ value also decreased 23.71% in structured fixed bed #1 in contrast to the fixed bed. The data agreed with the research from Nikolajsen[26], where similar composites were also applied in fixed bed for adsorption experiments. The reason for the phenomenon lies in the fact that the external surface area of adsorbents plays a pivotal role in mass transfer rate[27]. In other words, the larger external surface contributes to the higher mass transfer rate. Compared to the granular 5A zeolite, 5A zeolite/PSSF composites owned larger external surface, which was approximately the BET surface area of PSSF support -14 m^2/g. At the same time, intra-particle transport resistance was reduced by using the 5A zeolite/PSSF composites with the thickness of 1.5μm, which contributed to higher mass transfer rate as well. Hence, by adding 5A zeolite/PSSF composites with large external surface area in the outlet of the bed, the mass transfer rate was enhanced in the structured fixed bed #1. Finally, the bed utilization was enhanced. The LUB value of structured fixed bed #1, #2 and #3 was 35.71, 43.81 and 50.00m. This is due to the difference in intra-particle transport resistance of zeolite coatings. In other words, for the thicker zeolite coatings, it takes longer time for the gas molecule to diffuse from the surface to the inside.

Table 2. Length of unused bed (LUB) for methane adsorption in different fixed beds

Adsorption fixed beds	Inlet concentration (ppm)	Flow rate (mL/min)	LUB (mm)	ΔZ[a] (%)
Fixed bed	104	20	71.29	47.52
Structured fixed bed #1			35.71	23.81
Structured fixed bed #2			43.81	29.21
Structured fixed bed #3			50.00	33.33

a Relative to the percentage of LUB and L: $\Delta Z = \frac{LUB}{L} \times 100\%$, where L is the total bed length and LUB is the length of unused bed.

5. Conclusions

The paper-like sintered stainless-steel fibers (PSSF) support was fabricated by using wet lay-up papermaking technique. Moreover, 5A zeolite/PSSF composites were synthesized by using in situ hydrothermal synthesis using APTMS as a covalent linker and ion-exchange procedure. Adsorption dynamic experiments were used to compare the adsorption properties between the fixed bed filled with granular 5A zeolite and the structured fixed beds filled with granular 5A zeolite in the inlet and 5A zeolite/PSSF composites of different zeolite loading in the outlet of bed. The results indicated that bed pressure drop was reduced and mass transfer rate was enhanced in structured fixed bed. Thus, these features made the structured fixed bed a promising candidate to adsorb low-concentration methane from air. Furthermore, more work can be done to explore the parameters such as hydrothermal time, mole ratio of solution in LTA/PSSF composites' synthesis and its application in the structured fixed bed for adsorbing methane from air.

Acknowledgements

This work was financially supported by National Natural Science Foundation of China (Grant Nos: 21176086 and 21376101).

Notes and references

1. A. L. Mitchell, D. S. Tkacik, J. R. Roscioli, S. C. Herndon, T. I. Yacovitch, D. M. Martinez, T. L. Vaughn, L. L. Williams, M. R. Sullivan, C. Floerchinger, M. Omara, R. Subramanian, D. Zimmerle, A. J. Marchese and A. L. Robinson, *Environmental science & technology*, 2015, **49**, 3219-3227.
2. Y. Zhang, Z. Qin, G. Wang, H. Zhu, M. Dong, S. Li, Z. Wu, Z. Li, Z. Wu, J. Zhang, T. Hu, W. Fan and J. Wang, *Applied Catalysis B: Environmental*, 2013, **129**, 172-181.
3. T. E. Rufford, G. C. Y. Watson, T. L. Saleman, P. S. Hofman, N. K. Jensen and E. F. May, *Industrial & Engineering Chemistry Research*, 2013, **52**, 14270-14281.
4. T. A. Brady, M. Rostam-Abadi and M. J. Rood, *Gas Separation & Purification*, 1996, **10**, 97-102.
5. R. Bhargavi, K. Kadirvelu and N. Kumar, *International Journal of Environmental Sciences*, 2011, **1**, 938-947.
6. D. Das, V. Gaur and N. Verma, *Carbon*, 2004, **42**, 2949-2962.
7. P. Dwivedi, V. Gaur, A. Sharma and N. Verma, *Separation and Purification Technology*, 2004, **39**, 23-37.
8. B.-K. Chang, Y. Lu and B. J. Tatarchuk, *Chemical Engineering Journal*, 2006, **115**, 195-202.
9. H. Yang, D. R. Cahela and B. J. Tatarchuk, *Chemical Engineering Science*, 2008, **63**, 2707-2716.
10. B.-K. Chang, Y. Lu, H. Yang and B. J. Tatarchuk, *J. of Materi Eng and Perform*, 2006, **15**, 439-441.
11. H. Chen, H. Zhang and Y. Yan, *Industrial & Engineering Chemistry Research*, 2012, **51**, 16643-16650.
12. H. Chen, H. Zhang and Y. Yan, *Chemical Engineering Science*, 2014, **111**, 313-323.
13. K. Okada, H. Shinkawa, T. Takei, S. Hayashi and A. Yasumori, *Journal of Porous Materials*, 1998, **5**, 163-168.
14. V. Valtchev and S. Mintova, *Microporous and Mesoporous Materials*, 2001, **43**, 41-49.
15. S. Aguado, J. Gascon, D. Farrusseng, J. C. Jansen and F. Kapteijn, *Microporous and Mesoporous Materials*, 2011, **146**, 69-75.
16. A. Huang, F. Liang, F. Steinbach and J. Caro, *Journal of Membrane Science*, 2010, **350**, 5-9.
17. G. Guan, K. Kusakabe and S. Morooka, *Separation Science and Technology*, 2001, **36**, 2233-2245.
18. Y. Li, H. Zhou, G. Zhu, J. Liu and W. Yang, *Journal of Membrane Science*, 2007, **297**, 10-15.
19. Y. Li, H. Chen, J. Liu and W. Yang, *Journal of Membrane Science*, 2006, **277**, 230-239.
20. S. Mintova, S. Mo and T. Bein, *Chemistry of Materials*, 2001, **13**, 901-905.
21. J. L. Zuech, A. L. Hines and E. D. Sloan, *Industrial & Engineering Chemistry Process Design and Development*, 1983, **22**, 172-174.
22. J. Collins, 1967.
23. V. P. Valtchev, L. Tosheva and K. N. Bozhilov, *Langmuir : the ACS journal of surfaces and colloids*, 2005, **21**, 10724-10729.
24. S. N. Azizi, A. R. Dehnavi and A. Joorabdoozha, *Materials Research Bulletin*, 2013, **48**, 1753-1759.
25. D. Vu, M. Marquez and G. Larsen, *Microporous and Mesoporous Materials*, 2002, **55**, 93-101.
26. K. Nikolajsen, L. Kiwi-Minsker and A. Renken, *Chemical Engineering Research and Design*, 2006, **84**, 562-568.
27. E. Worch, *Adsorption technology in water treatment: fundamentals, processes, and modeling*, Walter de Gruyter, 2012.